DOI: 10.71568/daga2026.509

Towards an Analytical Model for Propeller Noise including Potential near field contributions

Jan W. Delfs
Institute of Aerodynamics and Flow Technology, DLR - German Aerospace Center
Lilienthalplatz 7, 38106 Braunschweig, Germany, Email: jan.delfs@dlr.de

Background

Propeller based propulsion for aircraft is the most promissing means for energy efficient flight. In the context of climate friendly ways of air transportation propeller aircraft have seen a renewed interest since the 2020ies. Moreover, related efforts towards electrical flight open the design space for unconventional aircraft. In particular, the use of electric motors, which -in contrast to gas turbines- allow for a much larger number of propellers as in conventional settings, enable favorable aerodynamic installations (e.g. augmentation of lift from propeller slip stream effects on the wings by distributed propulsion along the whole wing span). Aircraft design is characterized by extreme multi-disciplinary dependencies. Any discipline not taken into account at very early stages of design almost certainly leads to unwanted compromises. Traditionally, community noise, and even more so cabin noise cannot be taken into account in these early stages of preliminary- or even conceptual design. Here, high fidelity numerical noise simulations are not useful because a) hundreds of variations are to be expored and b) design details, e.g. the actual shape of propeller blades may not exactly be known yet. While the estimation of propeller community noise is relatively straight forward (farfield), the airborne cabin noise excitation (nearfield) is far more complex, see [1],[2]. Recently, handbook type ultra fast community noise prediction as well as a related ad-hoc nearfield model was presented in [3]. Here, a comprehensive, fully analytical propeller noise model is derived suitable to include tonal propeller related community-/cabin noise in early stages of a/c design.

Basic equation

The formulation of the problem starts with the Ffwocs-Williams and Hawkings equation for a solid (propeller) surface ∂V_B moving with a rigid body motion Mach number vector $\boldsymbol{M}_B = \boldsymbol{v}_B/a_\infty$ in a uniform stream of Mach number $\boldsymbol{M}_\infty = \boldsymbol{v}_\infty/a_\infty$ (windtunnel situation), with a_∞ the ambient speed of sound. FW-H's equation contains a volume source over the fluid around the propeller and two different propeller surface sources related to so called: a) loading noise, displayed below in blue and b) thickness noise, displayed in green. Typical in propeller noise theory the thickness noise integral is re-formulated to a volume integral over the propeller blade volume V_B and spatial derivatives are expressed as time derivatives. Initially three simplifying assumptions are made:

- neglect of volume sources (mostly active in the propeller streamtube immediately up- and downstream of the propeller plane
- neglect of viscous wakes behind the propeller
- neglect of effect of propeller tip vortices

These assumptions are justified because for the airborne propeller noise excitation of an aircraft fuselage, only the lateral development of the pressure field is of concern. With these assumptions the pressure fluctuation p' at a (fixed) observer position $\boldsymbol{x}$ and observer time t is

$$
\begin{aligned}
4\pi p'(\boldsymbol{x},t) = {} & \frac{1}{a_\infty}\frac{\partial}{\partial t}\int_{\partial V_B} \frac{(-\boldsymbol{\tau}+p'\boldsymbol{I})\boldsymbol{n}\cdot\big[C\boldsymbol{e}_r-\boldsymbol{M}_\infty\big]}{\big[CC_B+\boldsymbol{M}_B\cdot\boldsymbol{M}_\infty\big]\mu r}\,dS \\
& +\rho_\infty\frac{\partial^2}{\partial t^2}\int_{V_B}\frac{1-\big[CC_B+\boldsymbol{M}_B\cdot\boldsymbol{M}_\infty\big]}{\big[CC_B+\boldsymbol{M}_B\cdot\boldsymbol{M}_\infty\big]C\mu^2 r}\,dV \\
& +\int_{\partial V_B}\frac{(-\boldsymbol{\tau}+p'\boldsymbol{I})\boldsymbol{n}\cdot\big[(\boldsymbol{e}_r\cdot\boldsymbol{M}_\infty)\boldsymbol{M}_\infty+(\beta^2\boldsymbol{e}_r\big]C}{\big[CC_B+\boldsymbol{M}_B\cdot\boldsymbol{M}_\infty\big]\mu^2 r^2}\,dS \\
& +\frac{\partial}{\partial t}\int_{V_B}\Delta\boldsymbol{M}\cdot\frac{(\mu+3\boldsymbol{e}_r\cdot\boldsymbol{M}_\infty)\boldsymbol{M}_\infty+(\beta^2-2C(\boldsymbol{e}_r\cdot\boldsymbol{M}_\infty))\boldsymbol{e}_r}{(\rho_\infty a_\infty)^{-1}\big[CC_B+\boldsymbol{M}_B\cdot\boldsymbol{M}_\infty\big]\mu^3 r^2}\,dV \\
& +\int_{V_B}\Delta\boldsymbol{M}\cdot\frac{\big[\beta^2-2(\boldsymbol{e}_r\cdot\boldsymbol{M}_\infty)^2\big]\boldsymbol{M}_\infty-3\beta^2(\boldsymbol{e}_r\cdot\boldsymbol{M}_\infty)\boldsymbol{e}_r}{(\rho_\infty a_\infty^2)^{-1}(CC_B+\boldsymbol{M}_B\cdot\boldsymbol{M}_\infty)\mu^4 r^3}C\,dV,
\end{aligned}
\tag{1}
$$

where p' and $\boldsymbol{\tau}$ are the surface pressure fluctuation and the viscous stress tensor. A fat dot denotes the scalar product, $\boldsymbol{n}$ is the outward unit normal vector to the blade element dS. ρ_∞ is the ambient density, $r = |\boldsymbol{r}| = |\boldsymbol{x}-\boldsymbol{\xi}|$ and $\boldsymbol{e}_r := \boldsymbol{r}/r$ denote the distance and unit direction vector from each source point $\boldsymbol{\xi}(\tau)$ to the observer at $\boldsymbol{x}$. Moreover, $\beta = \sqrt{1-M_\infty^2}$ is the Prandtl-Glauert parameter.

$$
\mu = \big[(\boldsymbol{e}_r\cdot\boldsymbol{M}_\infty)^2+\beta^2\big]^{\frac{1}{2}} \tag{2}
$$

will turn out to be an important function to describe the convective change of distances, $C := \mu + \boldsymbol{e}_r\cdot\boldsymbol{M}_\infty$, $C_B := \mu - \boldsymbol{e}_r\cdot\boldsymbol{M}_B$, $\Delta\boldsymbol{M} = (\boldsymbol{M}_B - \boldsymbol{M}_\infty)$. As ususal, the integrands have to be evaluated at the retarded time $\tau = t - r^+/a_\infty$, where the convective distance $r^+ = r(\mu - \boldsymbol{e}_r\cdot\boldsymbol{M}_\infty)/\beta^2 = rC^{-1}$.

In eqn (1) the first two integrals correspond to those, which contribute to the farfield while the remaining 3 integrals are nearfield terms. Already at this stage one may observe that in contrast to the loading noise contribution to the nearfield, which scales with at most r^{-2}, there exists a thickness noise integral which scales with r^{-3}, which on top scales with the flight speed M_∞. This in turn means that very near the propeller the thickness noise dominates, i.e. for low cabin noise a highly loaded

blade is acceptable as long as it is thin (low thickness noise). Note, that this design requirement does not exist for community noise, since in the farfield both sources scale with r^{-1}.

A last simplification is the neglect of the effect of the angle of incidence of the propeller disk with respect to the freestream $\boldsymbol{M}_\infty$, i.e. $\boldsymbol{M}_\infty \cdot \boldsymbol{M}_B \approx 0$, because cabin noise is a topic of cruise flight, where this angle is small and hence any effect on the pressure field.

Next, according to classical propeller noise theory FW-H's eqn. (1) is evaluated for a single blade. A fixed and a co-rotatig co-ordinate system (superscript 0 and u respectively) is introduced with the axes orientated according to Fig. 1. Integrations are usefully carried out in the co-rotating system. First, at any given radial and circumferential position R, ϕ on the blade the normal component of the stress $\boldsymbol{f}_{s,p} = (p\boldsymbol{I} - \boldsymbol{\tau})\boldsymbol{n}|_{s,p}$ on the surface elements $dS_{s,p}$ on the suction (s) and on the pressure side (p) are combined to a resulting stress $\boldsymbol{f}(R,\phi) = (p\boldsymbol{I} - \boldsymbol{\tau})\boldsymbol{n}|_s + (p\boldsymbol{I} - \boldsymbol{\tau})\boldsymbol{n}|_p$. Then the surface integration is done only over the projection of the blade in the propeller plane (see grey domain in Fig.1), which is reasonable for slender blade profiles, because $dS_s(R,\phi) \approx dS_p(R\phi) \approx RdRd\phi/\cos\chi$, where $\chi(R)$ is the local pitch angle of the blade. Since the blade motion does not vary along the axial direction $\boldsymbol{e}_1$ the blade volume elements dV_B in the thickness noise integrals may be expressed as $dV \approx h(R,\phi)RdRd\phi/\cos\chi$, such that the volume integration reduces to the same blade planform as for the loading noise integral. The velocity of the volume elements is described by $\boldsymbol{v}_B(R,\phi) := \frac{1}{2}(\boldsymbol{v}_B|_s + \boldsymbol{v}_B|_p)$.

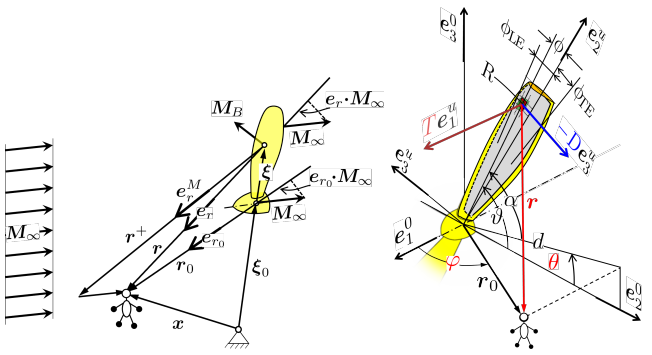

Figure 1: Nomenclature for propeller blade.

The propeller rotates with a constant shaft rotation frequency N_s in Hz, i.e. a circular shaft frequency of $\omega = 2\pi N_s$, so that the problem is periodic in time. In order to obtain the harmonics n of the propeller tones the pressure signal is decomposed into its Fourier components like $\hat{p}_n = \frac{\omega}{2\pi}\int_0^{2\pi/\omega} p'(t)\exp(-in\omega t)dt$. The loading noise component of the pressure field harmonics is

$$\hat{p}_{Ln}(\boldsymbol{x}) = \frac{\omega}{8\pi^2}\int_0^{\frac{2\pi}{\omega}}\int_0^{R_t}\int_{\phi_{\mathrm{TE}}}^{\phi_{\mathrm{LE}}} \exp(-in\omega t)\Big[\frac{ink\,\boldsymbol{e}_r^M\cdot\boldsymbol{f}}{\mu^2(\mu+\boldsymbol{e}_r\cdot\boldsymbol{M}_\infty)r} + \frac{\big[(\boldsymbol{e}_r\cdot\boldsymbol{M}_\infty)\boldsymbol{M}_\infty+\beta^2\boldsymbol{e}_r\big]\cdot\boldsymbol{f}}{\mu^3 r^2}\Big]_\tau \frac{R}{\cos\chi}dR\,d\phi\,d\tau, \quad (3)$$

in which $k = \omega/a_\infty$ is the shaft speed related wave number, and $\boldsymbol{e}_r^M = C\boldsymbol{e}_r - \boldsymbol{M}_\infty$. In a final step the normal stress $\boldsymbol{f}$ is split into a component in the direction of thrust T and into one in the direction of drag D ignoring radial stresses (see Fig.1), i.e $\boldsymbol{f} = -T\boldsymbol{e}_1^u + D\boldsymbol{e}_3^u = -T\boldsymbol{e}_1^0 - D\sin\vartheta\boldsymbol{e}_2^0 + D\cos\vartheta\boldsymbol{e}_3^0$. The thickness noise harmonics are

$$\hat{p}_{Tn}(\boldsymbol{x}) = \frac{\rho_\infty\omega a_\infty^2}{8\pi^2}\int_0^{\frac{2\pi}{\omega}}\int_0^{R_t}\int_{\phi_{\mathrm{TE}}}^{\phi_{\mathrm{LE}}} \exp(-in\omega t)\Big[-n^2k^2\frac{\Delta\boldsymbol{M}\cdot\boldsymbol{e}_r^M}{\mu^3C^2r} + ink\Delta\boldsymbol{M}\cdot\frac{(\mu_\infty+3\boldsymbol{e}_r\cdot\boldsymbol{M}_\infty)\boldsymbol{M}_\infty+(\beta^2-2C\boldsymbol{e}_r\cdot\boldsymbol{M}_\infty)\boldsymbol{e}_r}{\mu_\infty^4Cr^2} + \Delta\boldsymbol{M}\cdot\frac{\big[\beta^2-2(\boldsymbol{e}_r\cdot\boldsymbol{M}_\infty)^2\big]\boldsymbol{M}_\infty-3\beta^2(\boldsymbol{e}_r\cdot\boldsymbol{M}_\infty)\boldsymbol{e}_r}{\mu_\infty^5r^3}\Big]_\tau \frac{hR}{\cos\chi}dRd\phi d\tau \quad (4)$$

It is noted that the Fourier decomposition reduces the complexity of eqn (1) because the time derivatives of the integrals become explicit and because of the change of variables from the reception time integration in t to the retarded time τ, through $dt = \frac{CC_B+\boldsymbol{M}_B\cdot\boldsymbol{M}_\infty}{\mu C}d\tau$. All the variables marked in red in eqns (3 and 4) are periodic functions of the retarded time τ. This underlines the complexity of the nearfield effects, because in the farfield, only $\boldsymbol{f}$ and $\Delta\boldsymbol{M}$ are functions of τ. Note that the exponential still includes the observer time $t = \tau + r^+(\tau)/a_\infty$, in which the convective distance r^+ needs to be expressed in the retarded time τ.

Analytical solution of the Fourier decomposition

The evaluation of the terms in eqn(3 and 4) turn out quite cumbersome. The instantaneous distance r is obtained from

$$r_1 = r_0\cos\varphi$$
$$r_2 = d\cos\theta - R\cos\vartheta$$
$$r_3 = d\sin\theta - R\sin\vartheta$$
$$r = \sqrt{r_0^2 + R^2 - 2Rr_0\sin\varphi\cos\alpha} \quad (5)$$

Furthermore thanks to $\boldsymbol{r}\cdot\boldsymbol{M}_\infty = \boldsymbol{r}_0\cdot\boldsymbol{M}_\infty$. the unsteadiness in the expression $\boldsymbol{e}_r\cdot\boldsymbol{M}_\infty = \boldsymbol{e}_{r_0}\cdot\boldsymbol{M}_\infty(r/r_0)$ may be related to the one in the distance variable r. Now a convective distance variable $r^* := \mu r = r_0\sqrt{(\boldsymbol{e}_{r_0}\cdot\boldsymbol{M}_\infty)^2 + \beta^2(1 + r_s^2 - 2r_s\sin\varphi\cos\alpha)}$ may be defined, in which $r_s := R/r_0$. Since $\alpha = \omega\tau + \theta$ its rms value is $\tilde{r}^* = r_0\sqrt{(\boldsymbol{e}_{r_0}\cdot\boldsymbol{M}_\infty)^2 + \beta^2(1+r_s^2)}$, which allows to define the dimensionless convective nearfield distance variable

$$\nu_r := \frac{r^*}{\tilde{r}^*} = \sqrt{1 - \eta\cos\alpha} \quad (6)$$

with the convective position parameter

$$\eta := \frac{2r_s\beta^2\sin\varphi}{(1-\beta^2)\cos^2\varphi + \beta^2(1+r_s^2)} \quad (7)$$

Note that in the farfield $r_s \to 0$, so $\eta \to 0$ and thus $\nu_r = 1$. It is quite remarkable (not explicitly derived here) that all unsteady terms occuring in eqns (3, 4) may be expressed in negative and positive powers of ν_r (see eqns (11,12)), which is a one-parameter function (of η),

while covering any 3D position of an observer. Moreover, although there is no analytical Fourier decomposition in $\alpha = \omega\tau + \theta$ (or τ respectively) of powers of ν_r one may expand ν_r in powers of $\cos\alpha$ in closed form, while expressing the powers as harmonics m of α

$$\nu_r^p = \sum_{m=-\infty}^{\infty} \hat{\nu}_{r,m}^{(p)} \exp\left[im\alpha\right], \tag{8}$$

with

$$\hat{\nu}_{r,m}^{(p)} = \sum_{n=|m|,2}^{\infty} \left(\frac{\eta}{4}\right)^n \frac{\prod_{l=1}^{n}\left(2(l-1)-p\right)}{\left(\frac{n+m}{2}\right)!\left(\frac{n-m}{2}\right)!} \tag{9}$$

for any positve/negative integer power p; the 2 in the sum index is the step size of n. As an example Figure 2 shows these Fourier coefficients for ν_r and ν_r^{-3} respectively.

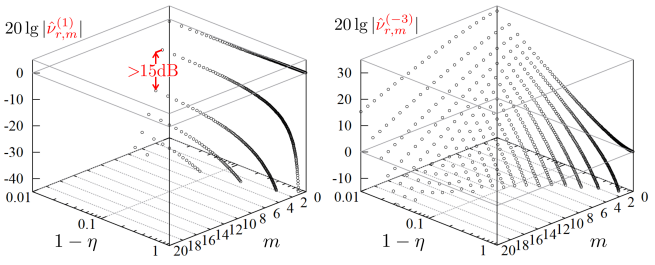

Figure 2: Fourier coefficients of ν_r and ν_r^{-3}.

It is noted that for each given η the first Fourier coefficient $\nu_{r,1}^{(1)}$ of ν_r strictly stays more than 15dB above all coefficients $m \geq 2$. This is important when expressing the reception time t in eqns (3,4) in terms of the retarded time through $r^+(\tau)$, which in turn is expressed in terms of ν_r. Representing the reception time t by only its zeroth and first Fourier coefficient of ν_r the time integration in (3) and (4) may be done analytically. For this purpose one uses the substitution $\omega\tau = \alpha + \theta - \phi$ and thus $d\tau = d\alpha/\omega$. Moreover using the relations $\int_0^{2\pi} e^{-i(n\alpha - s\cos\alpha)} d\alpha = 2\pi e^{in\pi/2} J_n(s)$ and $\int_0^{2\pi} e^{-i(n\alpha - s\cos\alpha)} \sin\alpha \, d\alpha = -\frac{2\pi n}{s} e^{in\pi/2} J_n(s)$ with J_n Bessel's function, one arrives at

$$\hat{p}_{(L,T)nB}(\boldsymbol{x}) = \sum_{m=-\infty}^{\infty} \hat{p}_{(L,T)nB}^{(m)}(\boldsymbol{x}), \tag{10}$$

with the loading noise contribution

$$\hat{p}_{LnB}^{(m)}(\boldsymbol{x}) = \frac{BR_t e^{-inB(\tilde{k}r_0 + \theta - \frac{\pi}{2})}}{4\pi r_0} \int_0^1 e^{-inB\left(kr_0 \frac{\nu_0\tilde{\mu} - \mu_\infty}{\beta^2}\right)} \times \int_{\phi_{\mathrm{TE}}}^{\phi_{\mathrm{LE}}} e^{inB\phi} \left\{ -\frac{inBM_\omega M_\infty TR^*}{\tilde{\mu}\beta^2} \hat{\nu}_{r,m}^{(-1)} - \frac{i}{\tilde{\mu}}\left[\frac{nBM_\omega \cos\varphi \, TR^*}{\tilde{\mu}\beta^2} - \frac{(nB \mp m)D}{\nu_1}\right] \hat{\nu}_{r,m}^{(-2)} - \frac{1}{\tilde{\mu}^2}\left[\frac{\cos\varphi \, TR^*}{\tilde{\mu}} - \frac{(nB-m)\beta^2 D}{nBM_\omega \nu_1}\right] \frac{R_t}{r_0} \hat{\nu}_{r,m}^{(-3)} \right\} d\phi \; J_{nB-m}\left(\frac{nBM_\omega R^* \sin\varphi \, \nu_1}{\tilde{\mu}}\right) \frac{1}{\cos\chi} dR^*, \tag{11}$$

and the thickness noise contribution

$$\hat{p}_{TnB}^{(m)}(\boldsymbol{x}) = \frac{\rho_\infty a_\infty^2 B e^{-inB(\tilde{k}r_0 + \theta - \frac{\pi}{2})}}{4\pi r_0} \int_0^1 e^{-inB\left(kr_0 \frac{\nu_0\tilde{\mu} - \mu_\infty}{\beta^2}\right)} \times \left\{ -\frac{nBM_\omega^2}{\beta^3}\left[\frac{nB-m}{(1+r_s^2)^{\frac{1}{2}}\nu_1} - \frac{nB\boldsymbol{e}_{r_0}\cdot\boldsymbol{M}_\infty}{(1+r_s^2)^{\frac{1}{2}}\tilde{\mu}} + \frac{nBM_\infty^2}{\tilde{\mu}^2\beta}\right] \hat{\nu}_{r,m}^{(-1)} + \frac{nBM_\omega M_\infty^2}{\tilde{\mu}^2\beta^2}\left[2nBM_\infty \frac{\boldsymbol{e}_{r_0}\cdot\boldsymbol{M}_\infty}{\beta^2} - i\frac{R_t}{r_0}\right] \hat{\nu}_{r,m}^{(-2)} + \left[\frac{M_\omega}{\tilde{\mu}^2}\left(\frac{nBM_\omega \boldsymbol{e}_{r_0}\cdot\boldsymbol{M}_\infty}{\beta^2} + i\frac{R_t}{r_0}\right)\left(\frac{nB-m}{\nu_1} - \frac{nB\boldsymbol{e}_{r_0}\cdot\boldsymbol{M}_\infty}{\tilde{\mu}}\right) - \frac{M_\infty^2 nBM_\omega \boldsymbol{e}_{r_0}\cdot\boldsymbol{M}_\infty}{\tilde{\mu}^3\beta^2}\left(\beta nBM_\omega \boldsymbol{e}_{r_0}\cdot\boldsymbol{M}_\infty + 2i\frac{R_t}{r_0}\right) - \frac{M_\infty^2}{\tilde{\mu}^3}\left(\frac{R_t}{r_0}\right)^2\right] \hat{\nu}_{r,m}^{(-3)} - \frac{3iM_\omega \boldsymbol{e}_{r_0}\cdot\boldsymbol{M}_\infty}{\tilde{\mu}_\infty^3}\frac{R_t}{r_0}\left[\frac{nB \mp m}{\nu_1} - \frac{nB\boldsymbol{e}_{r_0}\cdot\boldsymbol{M}_\infty}{\tilde{\mu}\beta^2}\right] \hat{\nu}_{r,m}^{(-4)} - \frac{3\beta \boldsymbol{e}_{r_0}\cdot\boldsymbol{M}_\infty}{\tilde{\mu}^4(1+r_s^2)^{\frac{1}{2}}}\left(\frac{R_t}{r_0}\right)^2\left[\frac{nB \mp m}{nB\nu_1} - \frac{\boldsymbol{e}_{r_0}\cdot\boldsymbol{M}_\infty}{\tilde{\mu}\beta^2}\right] \hat{\nu}_{r,m}^{(-5)} \right\} \int_{\phi_{\mathrm{TE}}}^{\phi_{\mathrm{LE}}} h e^{inB\phi} d\phi \; J_{nB-m}\left(\frac{nBM_\omega R^* \sin\varphi \, \nu_1}{\tilde{\mu}}\right) \frac{R^*}{\cos\chi} dR^*. \tag{12}$$

Herein R_t is the tip radius of the propeller, $M_\omega = kR_t$ denotes its circumferential tip Mach number, while $R^* := R/R_t$. In deriving eqns (10-12) from eqns (3-4) the description has been generalized from a one bladed propeller to one with B uniformly spaced blades. $\tilde{\mu} = \sqrt{(\boldsymbol{e}_{r_0}\cdot\boldsymbol{M}_\infty)^2 + \beta^2(1+r_s^2)}$ is the root mean square value of μ and μ_∞ is its value in the farfield $r_s \to 0$. Moreover, $\tilde{k} = k/(\mu_\infty + \boldsymbol{e}_{r_0}\cdot\boldsymbol{M}_\infty)$ is the convective wave number in the far field. The abbreviations $\nu_0 := \hat{\nu}_{r,0}^{(1)}$ and $\nu_1 := \frac{4}{\eta}|\hat{\nu}_{r,1}^{(1)}|$ were used with $\nu_{0|1} \to 1$ in the farfield.

Reduction of nearfield model for preliminary design input

The general propeller model eqns (10-12) requires the integration of the infinitesimal thrust force $T(\phi, R^*)d\sigma$ and drag force $D(\phi, R^*)d\sigma$ on each blade planform element $d\sigma = \cos^{-1}\chi R d\phi dR$ as well as the airfoil thickness distribution $h(\phi, R^*)$.

For the integration along the azimuth (blade chord) it is useful to define a mean chord line $\phi_0(R^*) = \frac{1}{2}(\phi_{TE} + \phi_{LE})$ and a relative azimuth $\phi^* = \phi - \phi_0$, so that $\exp(inB\phi) = \exp(inB\phi_0)\exp(inB\phi^*)$ and the integration changes like $\int_{\phi_{TE}}^{\phi_{LE}} \ldots d\phi \to \int_{-\Delta\phi}^{\Delta\phi} \ldots d\phi^*$ with $\Delta\phi = \frac{1}{2}(\phi_{LE} - \phi_{TE})$. This azimuthal distance $\Delta\phi$ of leading and trailing edge to the mean chord line may be expressed in terms of the local radius and chord of the blade planform element at R and l respectively, pitched by angle χ to yield $\tan\Delta\phi = 2R/(l\cos\chi)$.

Note that in eqns (11) and (12) the only variables depending on the azimuthal direction ϕ^* are T, D, h. In order to reduce the local loading and geometry information (which may not be available in preliminary a/c design) to global values one introduces average section stresses $\overline{T}^\phi$, $\overline{D}^\phi$ and mean section blade thickness $\overline{h}^\phi$. Then $\int_{-\Delta\phi}^{\Delta\phi}(T, D, h)\exp(inB\phi^*)d\phi^* \simeq (\overline{T}^\phi, \overline{D}^\phi, \overline{h}^\phi)\int_{-\Delta\phi}^{\Delta\phi}\exp(inB\phi^*)d\phi^*$. With that simplification the last integral may be done explicitly:

$\int_{-\Delta\phi}^{\Delta\phi}\exp(inB\phi^*)d\phi^* = \frac{2\sin(nB\Delta\phi)}{nB}$. This implies the definition of a compactness factor

$$\nu_c = \sin\left[nB\tan^{-1}\left(\frac{l}{2R}\cos\chi\right)\right] \tag{13}$$

Next the section thrust $\overline{T}^\phi$ and drag $\overline{D}^\phi$ have to be reduced to the propeller overall thrust and power coefficients c_T and c_P. For simplicity the section loads are assumed proportional to the square of the local circumferential speed and respective local aerodynamic coefficients as $(\overline{T}^\phi, \overline{D}^\phi) = \rho_\infty(2\pi N_s R_t)^2 R^{*2}(c_T^R, c_D^R)$, where N_s is the shaft rpm in s^{-1}. The overall thrust of the propeller is approximated by integration of $\overline{T}^\phi$ over the radius, multiplication with the average chord $\bar{l}$, and the number of blades B to be $\frac{1}{3}\rho_\infty B(2\pi N_s)^2 R_t^3 \bar{l}\overline{c_T^R}$ which according to the definition of the thrust coefficient c_T has to correspond to $\rho_\infty N_s^2(2R_t)^4 c_T$. Furtherly assuming that $c_T^R \approx \overline{c_T^R}$ one obtains

$$\overline{T}^\phi \approx \rho_\infty a_\infty^2 M_\omega^2 \frac{12}{\pi^2 B}\frac{R_t}{\bar{l}} R^{*2} c_T$$

with $M_\omega = 2\pi N_s R_t/a_\infty$. Likewise the overall torque of the propeller is approximated by integration of $(R\,\overline{D}^\phi)$ over the radius multiplied by $\bar{l}$ and summed for all B blades to be $\frac{1}{4}\rho_\infty B(2\pi N_s)^2 R_t^4 \bar{l}\overline{c_D^R}$ which according to the definition of the torque coefficient c_M has to correspond to $\rho_\infty N_s^2(2R_t)^5 c_M$. Furtherly assuming that $c_D^R \approx \overline{c_D^R}$ one obtains

$$\overline{D}^\phi \approx \rho_\infty a_\infty^2 M_\omega^2 \frac{16}{\pi^3 B}\frac{R_t}{\bar{l}} c_P,$$

where $c_P = c_M/(2\pi)$ is the power coefficient of the propeller. For slender aerofoils the mean section thickness $\overline{h}^\phi \approx \frac{1}{2}h^*_{\max}\bar{l}$ is reasonably approximated by half of the maximum airfoil thickness commonly expressed as aerofoil relative thickness $h^*_{\max}$.

After inserting the above approximations into eqn (11) the loading noise reads

$$\hat{p}^{(m)}_{LnB}(\boldsymbol{x}) = \frac{\rho_\infty a_\infty^2 M_\omega R_t^2 e^{-inB(\tilde{k}r_0+\theta-\frac{\pi}{2})}}{2\pi r_0}\times$$
$$\int_0^1 e^{-inB\left(kr_0\frac{\nu_0\tilde{\mu}-\mu_\infty}{\beta^2}-\phi_0\right)}\left\{-\frac{12iM_\omega^2 M_\infty c_T R^*}{\pi^2\beta^2}\hat{\nu}^{(-1)}_{r,m}\right.$$
$$-iM_\omega\left[\frac{12M_\omega\cos\varphi c_T R^*}{\pi^2\tilde{\mu}\beta^2}-\frac{16(nB\mp m)c_P}{\pi^3 nB\nu_1}\right]\hat{\nu}^{(-2)}_{r,m}$$
$$\left.-\frac{1}{nB\tilde{\mu}}\left[\frac{12M_\omega\cos\varphi c_T R^*}{\pi^2\tilde{\mu}}-\frac{16(nB-m)\beta^2 c_P}{\pi^3 nB\nu_1}\right]\frac{R_t}{r_0}\hat{\nu}^{(-3)}_{r,m}\right\}$$
$$J_{nB-m}\left(\frac{nBM_\omega R^*\sin\varphi\,\nu_1}{\tilde{\mu}}\right)\frac{\nu_c R^{*2}}{\tilde{\mu}\bar{l}\cos\chi}dR^*, \tag{14}$$

Note that now only pre-design parameters enter into the prediction of the loading noise harmonics. The integration over the radius is left for numerical evaluation. In contrast to the farfield expression, shown in [3] the integration cannot be approximated by the mean value theorem because here the argument of the Bessel functions may not be smaller than its order and thus may display oscillatory behavior.

Finally the same type of approximations as for the loading noise may be introduced in the thickness noise integral (12) to yield

$$\hat{p}^{(m)}_{TnB}(\boldsymbol{x}) = \frac{\rho_\infty a_\infty^2 B e^{-inB(\tilde{k}r_0+\theta-\frac{\pi}{2})}}{4\pi r_0}\int_0^1 e^{-inB\left(kr_0\frac{\nu_0\tilde{\mu}-\mu_\infty}{\beta^2}\right)-\phi_0}$$
$$\left\{-\frac{M_\omega^2}{\beta^3}\left[\frac{nB-m}{(1+r_s^2)^{\frac{1}{2}}\nu_1}-\frac{nB\boldsymbol{e}_{r_0}\cdot\boldsymbol{M}_\infty}{(1+r_s^2)^{\frac{1}{2}}\tilde{\mu}}+\frac{nBM_\infty^2}{\tilde{\mu}^2\beta}\right]\hat{\nu}^{(-1)}_{r,m}\right.$$
$$+\frac{M_\omega M_\infty^2}{\tilde{\mu}^2\beta^2}\left[2nBM_\infty\frac{\boldsymbol{e}_{r_0}\cdot\boldsymbol{M}_\infty}{\beta^2}-i\frac{R_t}{r_0}\right]\hat{\nu}^{(-2)}_{r,m}$$
$$+\left[\frac{M_\omega}{\tilde{\mu}^2}\left(\frac{nBM_\omega\boldsymbol{e}_{r_0}\cdot\boldsymbol{M}_\infty}{\beta^2}+i\frac{R_t}{r_0}\right)\left(\frac{nB-m}{nB\nu_1}-\frac{\boldsymbol{e}_{r_0}\cdot\boldsymbol{M}_\infty}{\tilde{\mu}}\right)\right.$$
$$-\frac{M_\infty^2 M_\omega\boldsymbol{e}_{r_0}\cdot\boldsymbol{M}_\infty}{\tilde{\mu}^3\beta^2}\left(\beta nBM_\omega\boldsymbol{e}_{r_0}\cdot\boldsymbol{M}_\infty+2i\frac{R_t}{r_0}\right)$$
$$\left.-\frac{M_\infty^2}{nB\tilde{\mu}^3}\left(\frac{R_t}{r_0}\right)^2\right]\hat{\nu}^{(-3)}_{r,m}$$
$$-\frac{3iM_\omega\boldsymbol{e}_{r_0}\cdot\boldsymbol{M}_\infty}{\tilde{\mu}^3_\infty}\frac{R_t}{r_0}\left[\frac{nB\mp m}{nB\nu_1}-\frac{\boldsymbol{e}_{r_0}\cdot\boldsymbol{M}_\infty}{\tilde{\mu}\beta^2}\right]\hat{\nu}^{(-4)}_{r,m}$$
$$\left.-\frac{3\beta\boldsymbol{e}_{r_0}\cdot\boldsymbol{M}_\infty}{nB\tilde{\mu}^4(1+r_s^2)^{\frac{1}{2}}}\left(\frac{R_t}{r_0}\right)^2\left[\frac{nB\mp m}{nB\nu_1}-\frac{\boldsymbol{e}_{r_0}\cdot\boldsymbol{M}_\infty}{\tilde{\mu}\beta^2}\right]\hat{\nu}^{(-5)}_{r,m}\right\}$$
$$h^*_{\max}\nu_c\bar{l}\,J_{nB-m}\left(\frac{nBM_\omega R^*\sin\varphi\,\nu_1}{\tilde{\mu}}\right)\frac{R^*}{\cos\chi}dR^*. \tag{15}$$

The expressions (14) and (15) reduce to the farfield formula given in [3] which was successfully validated with experimental data on two GE propellers of $2m$ diameter in a wide range of operating parameters. It is noted that the validity of the prediction extends up to the compactness limit, which is reached at $(nB)_{\text{crit}} = \pi/\tan^{-1}(l\cos\chi/(2R))$. Note that this limit does not depend on the circumferential tip Mach number of the propeller. Physically this indicates the harmonic number at which the circumferential periodicity length of the wave field becomes smaller than the chord length near the propeller tip. Beyond this harmonic the details of the loading and thickness distribution along the chord strongly influences the result; the simplifications introduced above become invalid.

Summary

Eqns (10,14,15) represent a model to predict propeller noise based on preliminary design information and generalizes a farfield model proposed in [3] to the nearfield.

Acknowledgement

The author gratefully acknowledges the support received by the German Research Foundation (DFG) within the Collaborative Research Center CRC TRR 364 (Project ID 498601949) and DLR for the funding of a research stay at Université de Sherbrooke, QC, Canada.

References

[1] Hanson, D.B.: Helicoidal Surface Theory for Harmonic Noise of Propellers in the Far-Field, AIAA Journal, Vol. 18, 1980, p. 1213.

[2] Near-Field Frequency-Domain Theory for Propeller Noise, AIAA-Journal Vol. 23, No.4, 1985, p. 499

[3] Delfs, J.W., Proskurov, S. Thoma, J., Langer, S.: A Propeller Noise Model for Aircraft Conceptual and Preliminary Design. To appear in CEAS Aeronautical Journal 2026.